Encapsulation of CdTe Quantum Dots into Synthetic Viral Capsids

Seiya Fujita and Kazunori Matsuura *
Department of Chemistry and Biotechnology, Graduate School of Engineering, Tottori University, 4-101 Koyama-minami, Tottori, 680-8552

Received <Month> <Date>, <Year>; CL-<No>; E-mail: < ma2ra-k@chem.tottori-u.ac.jp>)

Encapsulation behaviour of CdTe quantum dots with the size of 3 nm into synthetic viral capsid self-assembled from *β*-annulus peptide was analysed by using fluorescence correlation spectroscopy (FCS). At concentration above the critical aggregation concentration (CAC) of *β*-annulus peptide, diffusion time of encapsulated CdTe quantum dots in the synthetic viral capsid was estimated to be larger than that of free quantum dots.

Quantum dots such as CdTe and CdSe have attracted much attention due to their peculiar physical and chemical properties compared with that of bulk materials.[1] Based on the advantages of fluorescent brightness and stability, quantum dots have been applied as bioimaging nanoparticles. To give various function and biocompatibility, quantum dots encapsulated into polymers and liposomes have been developed.[2]

For the past decade, spherical viral capsids have attracted much attention as nanocarrier and nanoreactor, since they are natural supramolecular protein assembly with discrete nanospace.[3] For example, Douglas et al. reported synthesis of iron oxide nanoparticles with the size of 6-30 nm in the interior of Cowpea chlorotic mottle virus (CCMV).[4] Cornelissen et al. developed GFP-encapsulated CCMV via coiled-coil formation.[5] Encapsulation behavior of CdSe/ZnS into viral capsids such as brome mosaic virus andsimian virus 40 were also analyzed by transmission electron microscope (TEM) and dynamic light scattering (DLS).[6]

Recently, chemical strategies to rationally design artificial peptide and protein assemblies have been developed.[7] We have developed synthetic viral capsid self-assembled from 24-mer *β*-annulus peptide fragment (INHVGGTGGAIMAPV AVTRQLVGS) which participates in the formation of the dodecahedral internal skeleton of tomato bushy stunt virus.[8] The pH dependence of the *ζ*-potentials of synthetic viral capsid indicates that the C-terminal is directed toward the surface, while the N-terminal is directed toward the interior.[9] The C-terminal modification of *β*-annulus peptide enabled decoration of synthetic viral capsid with gold nanoparticles.[10a] We have also demonstrated that anionic dyes and DNA were encapsulated into the cationic interior of synthetic viral capsid.[9] By proper N-terminal modification, ZnO nanoparticles were also encapsulated into the capsid.[10b] The synthetic viral capsid has the advantage of reversible encapsulation by the concentration. The encapsulation behaviors were analyzed by TEM and equilibrium dialysis, however *in situ* analysis of the encapsulation behavior was not achieved.

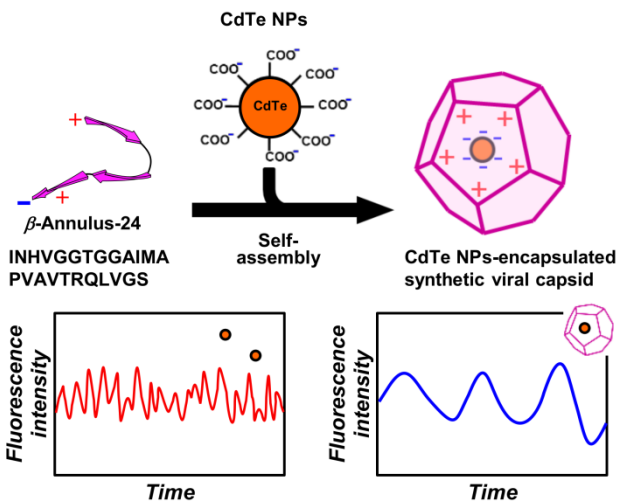

Figure 1. Schematic illustration of the encapsulation of CdTe NPs in synthetic viral capsid self-assembled from *β*-annulus peptide .

Here, we report in situ analysis of encapsulation behavior of CdTe quantum dots with the size of 3 nm into synthetic viral capsid by using fluorescence correlation spectroscopy (FCS). FCS is a technique in which spontaneous fluorescence intensity fluctuations are measured in a microscopic detection volume of about 10^{-15} L, provide information such as diameter and number of fluorescent nanoparticle.[11] Small, rapidly diffusing molecules produce rapidly fluctuating intensity patterns, whereas larger molecules produce more slowly fluctuating intensity patterns. We expected that the encapsulated CdTe NPs into synthetic viral capsid exhibit slower autocorrelation function decay due to the larger apparent diameter than free NPs. The encapsulation behavior of anionic CdTe NPs into the cationic interior of synthetic viral capsid formed by self- assembly of *β*-annulus peptide in 10 mM Tris-HCl buffer (pH 7.4) was investigated by FCS (Figure 1). Aqueous dispersion of CdTe NPs in the buffer was

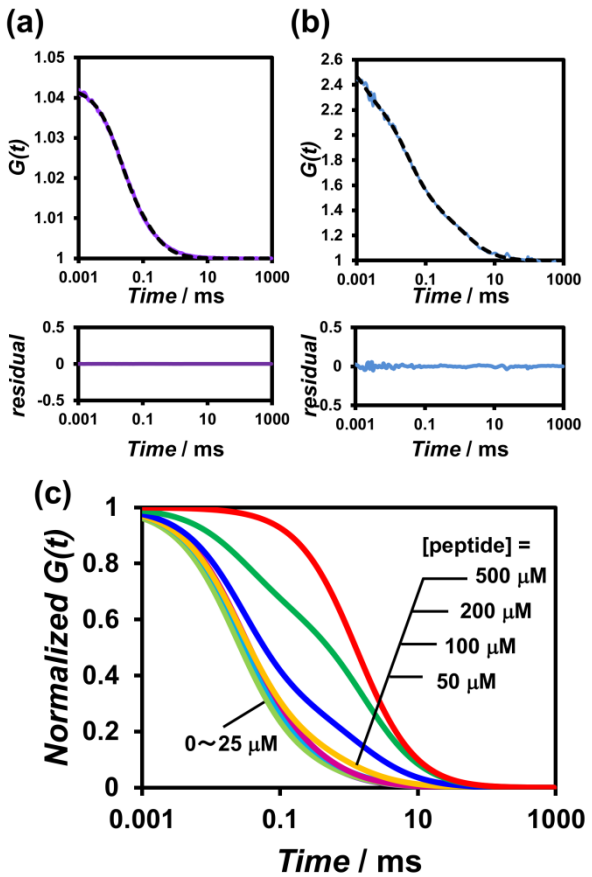

Figure 2. Measured (solid) and fitted (dot) autocorrelation curves for CdTe NPs (a) and mixture of CdTe and peptide (b) measured by fluorescence correlation spectroscopy . The lower graph shows residual plot. (c) Normalized autocorrelation curves of mixture of CdTe NPs (0.1 μM) and *β*-annulus peptide at [peptide] = 0-500 μM in 10 mM Tris-HCl buffer (pH 7.4) at 25 °C.

added to the dried peptide powder, and then the mixture was incubated for 1 h at 25 °C. Autocorrelation function (*G(t)*) of the aqueous dispersion of CdTe NPs alone showed simple sigmoidal decay curve (Figure 2a), which was fitted well to the theoretical equation of single component model (eq. 1),

$$G(t) = 1 + \frac{1}{N} \times \frac{y_1}{\left(1+\frac{t}{\tau_1}\right)\sqrt{1+\frac{1}{k^2}\frac{t}{\tau_1}}} \qquad (1)$$

where *N* is the average number of CdTe NPs in the detection area, *k* is the structural parameter, *y* is ratio of component, τ is diffusion time. In contrast, autocorrelation function (*G(t)*) of CdTe NPs in the presence of 100 μM *β*-annulus peptide showed two-step decay curve (Figure 2b), which was fitted to the dual component model (eq. 2).

$$G(t) = 1 + \frac{1}{N} \times \left(\frac{y_1}{\left(1+\frac{t}{\tau_1}\right)\sqrt{1+\frac{1}{k^2}\frac{t}{\tau_1}}} + \frac{y_2}{\left(1+\frac{t}{\tau_2}\right)\sqrt{1+\frac{1}{k^2}\frac{t}{\tau_2}}}\right) \qquad (2)$$

At peptide concentration of 50−200 μM, the residual (fitting deviation) in dual component model was smaller than that in single component model. From the result of curve-fitting, we can estimate the diffusion time and the ratio to be 0.0292 ms and 72 % for fast component, and 1.63 ms and 28% for slow component, respectively, which suggests co-existence of free and encapsulated CdTe NPs.

Figure 2c shows the autocorrelation function curve of CdTe NPs in the presence of various concentration of *β*-annulus peptide. At the concentration below 25 μM, the autocorrelation function showed single comportment curve with the diffusion time of about 0.08 ms. At the concentration 50 −200 μM, the autocorrelation function showed two-step decay curve, indicating co−existence of fast and slow components. At 500 μM, the autocorrelation function curve was fitted to single component model comprising of only slow component with the diffusion time of 1.31 ms. These results indicate that CdTe NPs were encapsulated into artificial viral capsid at the concentration above 50 μM, which is corresponding to the CAC of peptide (Figure S3).

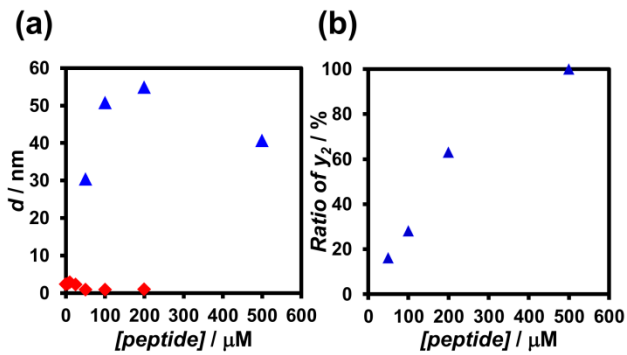

Figure 3. (a) *β*-annulus peptide concentration dependence of the apparent diameter of CdTe NPs determined by FCS curve fitting. Blue triangles stand for the slow component, and red squares stand for the fast component of CdTe NPs. Errors of the FCS measurements are estimated to be 21%. (b) Ratio of slower diffusing component determined by FCS curve fitting.

The apparent hydrodynamic diameters were calculated from by using Stokes-Einstein equation and the diffusion time of CdTe NPs determined by FCS curve fitting, and were plotted against the *β*-annulus peptide concentration as shown Figure 3a (see also Supporting information). Blue triangles stand for the slow component, and red squares stand for the fast component of CdTe NPs. The apparent diameters of fast component were estimated to be about 3 nm which is corresponding to the diameter of CdTe NPs, whereas that of slow component appeared above CAC of *β*-annulus peptide were estimated to be about 30-50 nm, which is similar to diameter of synthetic viral capsid. These result suggests that CdTe NPs were encapsulated in synthetic viral capsid at the concentration above CAC. Figure 3b indicates that the ratio of encapsulated CdTe NPs increased as the peptide concentration increased.

To confirm the encapsulation of CdTe NPs into synthetic viral capsids, CdTe NPs in the presence of *β*-annulus peptide observed by TEM stained with RuO_4 vapor.TEM image of 0.1 μM CdTe NP only showed nanospheres with the size of 3 nm

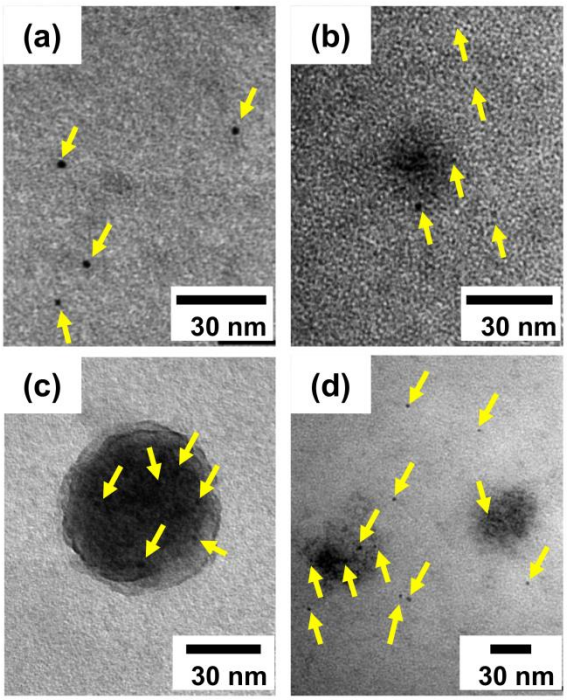

Figure 4. (a) Unstained TEM image of CdTe NPs at 0.1 μM. TEM image of CdTe NPs at 0.1 μM (b) 10 μM (c) 20 μM (d) in the presence of *β*-annulus peptide (100 μM). These samples were stained with 0.5% aqueous solution of ruthenium tetroxide. Arrow stands for position of CdTe NPs.

peptide, one CdTe NP was overlapped with the image of peptide assemblies stained with RuO_4 vapor with the size of about 30 nm (Figure 4b). Since the ideal aggregation number for dodecahedral assembly of *β*-annulus peptide is 60, the ratio of synthetic viral capsids and CdTe NPs is estimated to be 16.7 : 1 under the condition of Figure 4b. Therefore, one synthetic viral capsid would statistically encapsulated only one NP in the condition of FCS measurement. TEM image of 0.1 μM CdTe NPs in the presence of 500 μM *β*-annulus peptide also showed that one peptide nanocapsule encapsulated only one NP, whereas in the presence of 25 μM *β*-annulus peptide, any peptide assemblies were not observed (Figure S5), which are comparable to the FCS results. TEM image of 10 μM CdTe NPs in the presence of *β*-annulus peptide showed that many CdTe NPs overlapped with the image of peptide assemblies, and NPs outside the capsid minimally observed (Figure 4c), suggesting that almost NPs are encapsulated[12]. TEM image of 20 μM CdTe NPs in the presence of *β*-annulus peptide showed not only encapsulated CdTe NPs , but also free CdTe NPs.

In conclusion, we have analyzed *in situ* encapsulation behavior of CdTe quantum dots with size of 3 nm into artificial viral capsid self-assembled from *β*-annulus peptide by using FCS and TEM. At concentration above CAC, FCS curves of mixture of CdTe NPs and peptide showed increased of diffusion time of CdTe NP. FCS Curves of mixture of CdTe NPs and *β*-annulus peptide were fitted with dual component model, indicating co-exitence of free and encapsulated CdTe NP. The apparent diameters of slow component appeared above CAC were estimated to be about 30-50 nm, which is similar to diameter of synthetic viral capsid. TEM image of CdTe NPs in the presence of *β*-annulus peptide showed that CdTe NPs were encapsulated in synthetic viral capsid. This study gave encapsulation efficiency of guest molecules into artificial viral capsid in water. This result will help containing guest molecules such as drug.

This research was partially supported by The Canon Foundation and a Grant-in-Aid for Scientific Research (B) (No. 15H03838) from the Japan Society for the Promotion of Science (JSPS).

References and Notes

1 a) A. P. Alivisatos, *J. Phys. Chem.*, **1996**, *100*, 13226. b) T. Trindade, P. O'Brien, N. L. Pickett, *Chem. Mater.*, **2001**, *13*, 3843.

2 a) C. E. Probst, P. Zrazhevskiy, V. Bagalkot, X. H. Gao, *Adv. Drug Deliv. Rev.*, **2013**, *65*, 703. b) K. D. Wegner, N. Hildebrandt, *Chem. Soc. Rev.*, **2015**, *44*, 4792.

3 a) T. Douglas, M. Young, *Science*, **2006**, *312*, 873. b) N. F. Steinmetz, T. Lin, G. P. Lomonossoff, J. E. Johnson, *In Viruses and Nanotechnology*, ed by M. Manchester, N. F. Steinmetz, Springer-Verlag, Berlin, **2009**, Vol. *327*,pp 23-58 . c) A. A. A. Aljabali, F. Sainsbury, G. P. Lomonossoff, D. J. Evans, *Small*, **2010**, *6*, 818. d) L. M. Bronstein, *Small*, **2011**, *7*, 1609.

4 T. Douglas, E. Strable, D. Willits, A. Aitouchen, M. Libera, M. Young, *Adv. Mater.*, **2002**, *14*, 415.

5 I. J. Minten, L. J. A. Hendriks, R. J. M. Nolte, J. J. L. M. Cornelissen, *J. Am. Chem. Soc.*, **2009**, *131*, 17771.

6 a) S. K. Dixit, N. L. Goicochea, M. C. Daniel, A. Murali, L. Bronstein, M. De, B. Stein, V. M. Rotello, C. C. Kao, B. Dragnea, *Nano Lett.*, **2006**, *6*, 1993. b) D. Gao, Z. P. Zhang, F. Li, D. Men, J. Y. Deng, H. P. Wei, X. E. Zhang, Z. Q. Cui, *Int. J. Nanomed.*, **2013**, *8*, 2119.

7 a) K. Matsuurua, *RSC Adv.*, **2014**, *4*, 2942. b) B. E. I. Ramakers, J. C. M. Hest, D. Lowik, *Chem. Soc. Rev.* **2014**, *43*, 2743.

8 a) K. Matsuura, K. Watanabe, T. Matsuzaki, K. Sakurai, N. Kimizuka, *Angew. Chem. Intl. Ed.*, **2010**, *49*, 9662. b) K. Matsuura, *Polymer J.*, **2012**, *44*, 469.

9 K. Matsuura, K. Watanabe, Y. Matsushita, N. Kimizuka, *Polymer J.*, **2013**, *45*, 529.

10 a) K. Matsuura, G. Ueno, S. Fujita, *Polymer J.*, **2015**, *47*, 146. b) S. Fujita, K. Matsuura, *Nanomaterials*, **2014**, *4*, 778.

11 a) S. T. Hess, S. H. Huang, A. A. Heikal, W. W. Webb, *Biochemistry*, **2002**, *41*, 697. b) W. Al-Soufi, B. Reija, S. Felekyan, C. A. M. Seidel, M. Novo, *ChemPhysChem.*, **2008**, *9*, 1819. c) C. S. Chen, J. Yao, R. A. Durst, *J. Nanopart. Res.*, **2006**, *8*, 1033. d) M. Comas-Garcia, R. F. Garmann, S. W. Singaram, A. Ben-Shaul, C. M. Knobler, W. M. Gebart, *J. Phys. Chem. B*, **2014**, *118*, 7510.

12 We could not obtain any analyzable autocorrelation function curve from FCS measurement at [CdTe] = 10 μM. In general, suitable fluorophore concentration for FCS measurement is 1 nM ~ 100 nM. At the concentration range, the signal fluctuations from fluorophores diffusing in the focal volume are large enough to yield good signal-to-noise ratio.